Applied Geochemistry 161 (2024) 105879

Contents lists available at ScienceDirect

Applied Geochemistry

journal homepage: www.elsevier.com/locate/apgeochem

The role of alkalinity on metals removal from petroleum produced water by dolomite

Khalid Omar, Javier Vilcáez *

Boone Pickens School of Geology, Oklahoma State University, Stillwater, OK, 74078, USA

ARTICLE INFO

Editorial handling by: Dr Daniel S. Alessi

Keywords:
Petroleum produced water
Dolomite
Toxic metals
Alkalinity
Precipitation
Sorption

ABSTRACT

Alkalinity is a critical parameter for describing the composition, pH buffer capacity, and precipitation potential of petroleum produced water (PW). Besides salinity, alkalinity and metal concentrations are generally greater in PW than in freshwater (FW) and seawater. This study presents batch reaction experimental and simulation results showing that the removal of Ba, Sr, and Cd from PW by dolomite is mostly due to sorption reactions, with sorption reactions and thus removal levels being higher for Cd than for Ba and Sr. In contrast, we found that the removal of Pb and As from PW by dolomite is largely due to precipitation and coprecipitation reactions of carbonate minerals on dolomite. Analyses of changes in the morphology as well as in the elemental and mineral composition of dolomite surface, along with pH, alkalinity, and Ba, Sr, Cd, Pb, and As removal measurements using synthetic PW and FW containing high concentrations (~100 mg/L) of single and mixture toxic metals and metalloids (Ba, Sr, Cd, Pb, and As) at different initial alkalinity and pH conditions, indicate that in addition to salinity, alkalinity and pH generated from the dissolution of dolomite controls the removal of Ba, Sr, Cd, Pb, and As from PW by dolomite. However, we found that their impact is different for each metal in PW and FW. Ba, Sr, and Cd removal by dolomite is 10, 2, and 4 times smaller in PW than in freshwater (FW), respectively. Whereas As removal is practically the same regardless of salinity. Moreover, this study reveals the need of thermodynamic data of complex carbonate minerals formed from the precipitation of Ba, Sr, Cd, Pb, and As to capture the effect of alkalinity on their removal from PW by dolomite.

1. Introduction

Conventional and unconventional oil and gas industries produce huge amounts of wastewater, commonly called produced water (PW). This wastewater is characterized by high concentrations of total dissolved solids (TDS), dissolved organic matter such as hydrocarbons, and dissolved gases such as carbon dioxide and hydrogen sulfide. TDS mainly consists of chlorine, carbonate, sulfate, and hydroxide salts of heavy metals, metalloids, and alkaline earth metals, as well as naturally occurring radioactive materials (NORM). The concentration of heavy metals, metalloids, and alkaline earth metals in PW can be orders of magnitude higher than in shallow groundwater and seawater. Their concentrations greatly exceed the maximum contaminant levels (MCLs) of drinking water standards imposed by the U.S. Environmental Protection Agency (EPA). Therefore, to prevent the contamination of surface and underground sources of drinking water (USDW) and for economic motives, PW is usually disposed into deep saline aquifers. However, the injection of huge volumes of PW into geologic units induces seismicity episodes even in regions that are not tectonically active, raising the prospect of USDW contamination due to the possible upward migration of PW through induced or naturally occurring faults, fractures, and abandoned wells.

To prevent the risk of USDW contamination, in previous studies we investigated the fate and transport of a representative toxic metal (Ba) in dolomite saline aquifers (Ebrahimi and Borrok, 2020; Ebrahimi and Vilcáez, 2018a, 2018b, 2019; Vilcáez, 2020) as well as the feasibility of using dolomite as filtration media to remove toxic heavy metals, alkaline earth metals, and metalloids from PW (Omar and Vilcáez, 2022). Different from previous studies which focused on relatively low concentrations (<1 mg/L) of toxic metals (e.g., Zn, Cu, and As (V)) commonly present in shallow groundwater systems (TDS <1000 mg/L), our studies focus on the reactive transport of high concentrations (~100 mg/L) of toxic heavy metals, alkaline earth metals, and metalloids commonly present in PW (TDS = 40,000–120,000 mg/L). The results of our previous studies suggest that the competition of cations for hydration sites of dolomite and complexation reactions of metals and chlorine

* Corresponding author.
E-mail address: vilcaez@okstate.edu (J. Vilcáez).

https://doi.org/10.1016/j.apgeochem.2023.105879
Received 1 June 2023; Received in revised form 15 November 2023; Accepted 18 December 2023
Available online 23 December 2023

Table 1
Initial composition of the synthetic produced waters (PW) used for experiments.

(mg/L)	Type of produced water (PW)						
	I	II	III	IV	V	VI	VII
Na	15,647.2	17,667.5	18,538.3	18,211.5	17,802.2	17,740.2	18,112.0
Cl	29,996.7	31,305.7	33,926.7	31,656.0	31,070.0	29,385.5	29,938.5
Ca	4074.9	4388.2	4520.9	4424.2	4796.7	4663.8	4445.6
Mg	9,41.96	1020.1	1045.0	1047.9	1039.8	1077.0	1023.7
Ba	92.31					87.88	94.13
Sr		95.0				97.65	98.09
Cd			72.68			68.21	88.47
Pb				85.64		85.64	95.11
As					99.26	91.98	105.25
Alkalinity	11.28	12.16	11.07	16.45	58.42	98.86	0.00[a]
pH	8.25	8.88	7.98	6.63	6.81	6.64	2.39

[a] Below detection limit.

ions control the removal of toxic metals from PW by dolomite. Moreover, they revealed higher removal levels of Pb and Cd than Ba, Sr, and As, as well as a different affinity sequence of Ba and Sr at high and low salinity levels (Brown and Parks, 2001; Omar and Vilcáez, 2022). However, the role of alkalinity and dolomite dissolution on toxic metals and metalloids removal from PW has not been assessed before. Alkalinity is a critical parameter for describing the composition, pH buffer capacity, and precipitation potential (scaling) of waters from the oil and gas industry (Kaasa and Østvold, 1996). Water alkalinity is the equivalent sum of the bases that are titratable with strong acids (Stumm and Morgan, 1996). In most natural waters, alkalinity is the sum of $m\mathrm{HCO}_3^-$ and $2m\mathrm{CO}_3^{2-}$ ions because they are the predominant anions compared to other anion species such as OH^- (Drever, 1997).

Alkalinity concentrations are generally greater in PW than in freshwater (FW). For instance, the alkalinity of FW (TDS of 105–931 mg/L) and brackish water (TDS of 1037–6900 mg/L) in Oklahoma is typically around 20–250 mg/L (Ribeiro et al., 2021), whereas alkalinity concentrations in PW from conventional natural gas, conventional oil, shale gas, and coal-bed methane deposits in the continental U.S. has been reported to be 0–285 mg/L, 300–380 mg/L, 160–188 mg/L, and 55–9450 mg/L, respectively (Alley et al., 2011). Considering the relatively high concentrations of alkalinity in PW, and that dolomite dissolution has been reported as an important factor in the formation of new minerals (Holail and Al-Hajari, 1997; Ingles and Anadon, 1991; Ryan et al., 2019; Verrecchia and Le Coustumer, 1996), the possibility of precipitation and/or coprecipitation of toxic heavy metals, alkaline earth metals, and metalloids present in PW as carbonate minerals on dolomite cannot be discarded. Several studies have been conducted to understand the precipitation of metals as carbonate minerals from seawater (Brown and Parks, 2001) and freshwater (Alexandratos et al., 2007; Da'ana et al., 2021; Jensen, 2020; Lin et al., 2013; Tesoriero and Pankow, 1996) in different rock and soil materials. From those studies, it is known that carbonate mineral precipitates (e.g., calcite, magnesite, and siderite) can incorporate trace metal cations from seawater and that carbonate minerals precipitation can effectively sequester As from groundwater, for instance. Many other studies have focused on microbial-induced carbonate minerals precipitation (Chen et al., 2021; Kumari et al., 2016). It is known from those studies that bio-precipitation of carbonates can result in the elimination of Pb, Sr, and Cd from freshwater (Kim et al., 2021). Considering this information, we hypothesize that in addition and/or in parallel to sorption reactions, and depending on the pH and alkalinity, precipitation and/or coprecipitation reactions can contribute to the removal of toxic metals, alkaline earth metals, and metalloids as carbonate minerals from PW in natural or artificial dolomite porous media. This includes deep dolomite aquifers where PW is commonly disposed as well as engineered filters made of dolomite grains. PW can be pretreated for dissolved oil hydrocarbons by stimulating the activity of indigenous anaerobic oil degrading microbial communities that are adapted to high salinity conditions (Ezennubia and Vilcáez, 2023).

To elucidate the role of alkalinity and dolomite dissolution on Ba, Sr, Cd, Pb, and As removal from PW by dolomite, we conducted batch reaction experiments using synthetic PW and FW of different alkalinity and Ba, Sr, Cd, Pb, and As content but same Ca, Mg, and NaCl content. The approach consisted of analyzing changes in the morphology as well as in the elemental and mineral composition of the dolomite surface due to precipitation/dissolution sorption/desorption reactions. For the sake of simplicity, the toxic heavy metals, alkaline earth metals, and metalloids studied in this study (Ba, Sr, Cd, Pb, and As) are called toxic metals from this point on in this article.

2. Materials

2.1. Dolomite

Dolomite was collected from the Arbuckle Group outcrop in southwest Missouri. The dolomite samples were analyzed via Powder X-ray Diffractometer (Bruker XRD D8 ADVANCE Plus). The results confirmed that samples were composed of 98% dolomite and 2% of both blocky calcite cement and amorphous silica. The XRD spectrum distinguished dolomite-structure (JCPDS: 79–1342) from calcite-structure (JCPDS: 86–2334) minerals. The XRD spectra from collected samples displayed the highest intensity of 104 (>2500 counts) at 31^o 2 Θ as well as strong dolomite cation (e.g., Mg and Ca) ordering peaks (101, 015, and 021 at 22^o 2Θ, 35^o2Θ, and 44^o2Θ, respectively) confirming that the samples were near perfect dolomite and suggesting that the collected dolomite had near stochiometric composition (Mg/Ca1) (Fig. S1).

2.2. Dolomite grains

The collected dolomite was crashed and sieved multiple times to obtain dolomite grains of uniform size (300–600 μm). The obtained dolomite grains were washed with ultrapure deionized water in an ultrasonic bath to remove dust particles from the grain surfaces. Then, the dolomite grains were dried at room temperature and characterized by XRD and SEM analyses.

2.3. Synthetic produced water

Produced water has very complex chemistry and a detailed compositional analysis is quite challenging due to its high TDS content (Emmons et al., 2022). Since TDS in PW is mostly composed of chloride and carbonate salts, synthetic PW of different alkalinity (HCO_3^- and CO_3^{2-}) and toxic metals content but the same Ca, Mg, and NaCl content was prepared by adding NaCl, $\mathrm{CaCl_2.2H_2O}$, $\mathrm{MgCa_2.6H_2O}$, $\mathrm{SrCa_2.6H_2O}$, $\mathrm{BaCa_2.2H_2O}$, $\mathrm{CdH_8N_2O_{10}}$, $\mathrm{PbCl_2}$, and $\mathrm{AsCl_3}$ (Fisher Scientific Co. with the purity of >99.9%) to ultrapure deionized water (Table S1). TDS of the prepared synthetic PW was 68,000–75,000 mg/L. To determine the

Table 2
Initial composition of the synthetic freshwaters (FW) used for experiments.

(mg/L)	Type of freshwater (FW)						
	I	II	III	IV	V	VI	VII
Na	26.58	24.92	27.15	26.42	23.98	26.00	26.89
Cl	235.55	272.17	185.42	219.77	344.54	431.17	535.75
Ca	42.87	42.54	39.42	41.35	43.80	107.25	41.96
Mg	10.77	12.12	11.08	10.89	12.50	10.51	11.57
Ba	96.65					97.81	98.73
Sr		97.40				100.79	100.89
Cd			95.29			90.51	97.93
Pb				90.71		0.20	100.67
As					105.18	104.12	103.59
Alkalinity	2.39	4.22	2.20	3.86	0.00	15.29	0.00[a]
pH	6.41	5.89	5.63	5.30	2.58	6.36	2.57

[a] Below detection limit.

effect of salinity, synthetic freshwater (FW) was prepared and used to conduct the same experiments as with synthetic PW. Total dissolved solids of the prepared synthetic FW was <2000 mg/L and contained the same salts as the synthetic PW (Table S2). The initial alkalinity of the prepared synthetic PW and FW, that results from the dissolution of atmospheric CO_2, was increased by adding $CaCO_3$. The prepared synthetic PW and FW were stirred for 24 h, and possible undissolved particles in the prepared synthetic PW and FW were removed by filtration using a 0.4 μm cellulose filter.

Seven types of synthetic PW and FW were prepared. PW and FW types I–V contained only one toxic metal, and they were all added with $CaCO_3$ to increase alkalinity. PW and FW type VI contained all toxic metals, and they were added with $CaCO_3$ to increase alkalinity, whereas PW and FW type VII contained all toxic metals, but they were not added with $CaCO_3$ to increase alkalinity (Tables S1 and S2). The resulting concentrations of Ca and Mg in the synthetic PW correspond to PW in Oklahoma (Ribeiro et al., 2021) and U.S. Mid Continent (Guerra et al., 2011). Concentrations of sulfate in PW are negligible in these regions. Therefore, the prepared synthetic PW and FW did not contain dissolved sulfate. Arsenite (As(III)) salt ($AsCl_3$) was used instead of arsenate (As (V)) because PW originates under reduced conditions and the oxidation of arsenite to arsenate by dissolved oxygen is very slow (Dixit and Hering, 2003). For comparisons, we added 100 mg/L of each toxic metal to the prepared synthetic PW and FW. However, due to their different solubility the resulting dissolved concentrations of each toxic metal were different as shown in Tables 1 and 2. The used concentrations of Ba, Sr, Cd, Pb, and As correspond to reported concentrations in PW. Their concentrations range between a few to hundred mg/L (Guerra et al., 2011).

3. Methods

3.1. Batch experiments

Tables 1 and 2 show the measured alkalinity, initial pH, and composition of all types of synthetic PW and FW used to conduct the batch reaction experiments. All experiments were conducted in duplicate. An amount of 100 mL of each type of synthetic PW or FW was added to 250 mL flasks containing 40 g of dolomite grains. The flasks were placed in an orbital shaking incubator operating at 80 orbits/min. Temperature was fixed at 25 °C. Samples of 1.5 mL were carefully taken hourly for 72 h, and their composition was analyzed at the Soil, Water, and Forage Analytical Laboratory (SWFAL) of Oklahoma State University (OSU). The analysis included the measurement of all heavy metals, alkaline earth metals, and metalloids (Na, Ca, Mg, Ba, Sr, Cd, Pb, and As), chloride (Cl^-), as well as pH, and alkalinity (HCO_3^- and CO_3^{2-}). The concentration of Na, Ca, Mg, Ba, Sr, Cd, Pb, and As were measured by ICP-OES analysis. Alkalinity was measured by the titration method using a Hach TitraLab AT1000 Series auto-titrator with an autosampler. This method involves the titration of samples with standard 0.02N sulfuric acid (H_2SO_4) titrant to endpoints of pH 8.3 and 4.5. The pH endpoint of 8.3 corresponds to carbonate alkalinity, whereas the pH endpoint of 4.5 corresponds to bicarbonate alkalinity. Chloride was measured by the colorimetric method using ferricyanide in a flow-injection analyzer (Ballinger, 1979; Federation and Aph Association, 2005). Once an equilibrium condition was reached, reflected by a constant pH, dolomite grains were collected and then analyzed by XRD and SEM-EDS analyses to determine changes in the morphology as well as the elemental and mineral composition of the dolomite surface due to precipitation/dissolution and sorption/desorption reactions.

3.2. Surface morphology and composition analyses

In addition to sorption reactions, precipitation reactions are known to also result in the removal and thus retardation of toxic metals transport in groundwater. Precipitation reactions can sequester toxic metals into carbonate, silicate, and sulfate mineral, and/or salt phases. Precipitation reactions occur when the aqueous phase solution reaches saturation with respect to mineral phases. In natural carbonate systems, scavenging metals as a carbonate phase occurs through direct precipitation and/or dissolution/precipitation reactions controlled by thermodynamic and kinetic factors (Balci et al., 2018; Thompson and Ferris, 1990; Thompson et al., 1997). Phases of calcium carbonate, for instance, in surface and subsurface environments range from amorphous to crystalline, and from anhydrous (e.g., calcite, aragonite, and vaterite) to hydrated (e.g., monohydrocalcite ($CaCO_3{\cdot}H_2O$) and ikaite ($CaCO_3{\cdot}6H_2O$)) phases (Anthony et al., 2007; Fukushi et al., 2011). Precipitation of carbonate mineral phases along with sorption reactions can result in changes in the morphology and elemental composition of dolomite surface which in turn can result in changes in the removal of toxic metals by dolomite. The method we used to determine precipitation reactions due to the changes in the composition of the aqueous phase was SEM imaging. The method we used to determine the amorphous or crystal structure of precipitates as well as the changes in the mineral composition of dolomite consisted of X-ray Powder Diffraction (XRD) analysis (Wei et al., 2003). The method we used to determine changes in the elemental composition of dolomite surface due to precipitation and sorption reactions of toxic metals consisted of Scanning Electron Microscopy-Dispersive X-ray Spectroscopy (SEM-DES) analyses (Alexandratos et al., 2007). The removal of toxic metals from PW and FW was determined by Inductively Coupled Plasma-Optical Emission Spectroscopy (ICP-OES) analysis of metals in the aqueous phase. High-resolution XRD analyses were conducted on pulverized dolomite grains at the OSU Microscopy Laboratory using a Bruker D8 ADVANCE Plus XRD instrument. The obtained XRD data were semi-quantitatively analyzed via DIFFRAC.EVA software. Dolomite samples were dried but not pulverized for SEM-EDS analysis. This analysis was performed at the OSU Microscopy Laboratory using a SEM FEI Quanta 600 field emission

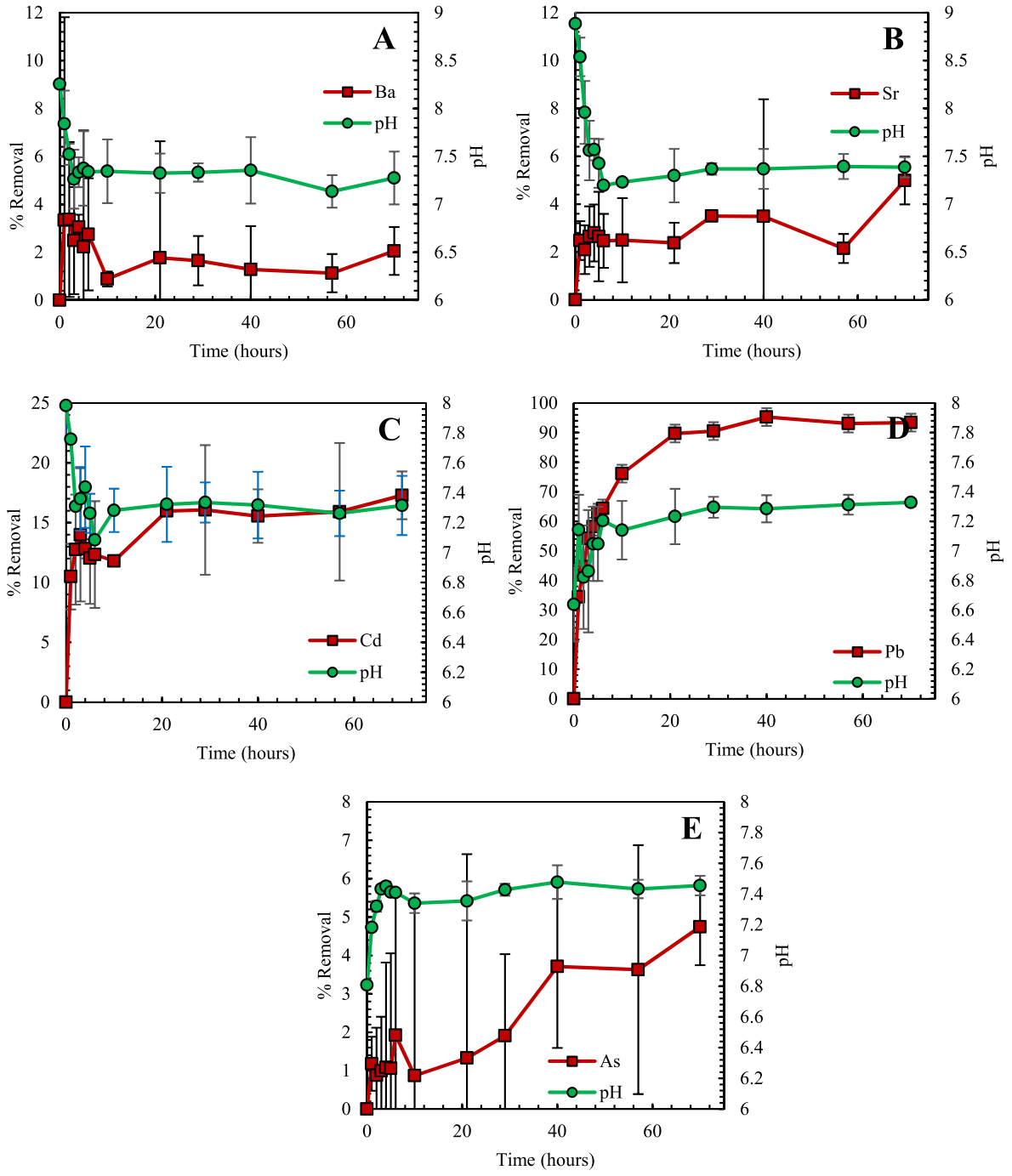

Fig. 1. Batch reaction experiment results of single metals removal by dolomite from PW: A) Ba (PW type I); B) Sr (PW type II); C) Cd (PW type III); D) Pb (PW type IV); and E) As (PW type V).

gun ESEM with Bruker EDS and HKL EBSD. Samples for SEM-EDS analysis were coated with carbon (graphite) to prevent artifacts and to optimize the quality of the images. SEM-EDS mapping of elements was performed at different magnification scales (e.g., 1 mm, 100 μm, and 10 μm). XRD and SEM-EDS analyses were done on dolomite grains collected at the beginning and end of the batch experiments.

4. Results and discussion

4.1. Batch reaction experiments

Batch reaction experiments were conducted to measure pH, alkalinity, and concentration profiles of toxic metals in solution over time, as well as to analyze changes in the mineral and elemental composition of dolomite grains at the end of each batch experiment. Experiments were conducted using synthetic PW and FW of different initial compositions (Tables 1 and 2) until an equilibrium condition reflected by a constant pH was reached.

Fig. 1 shows Ba, Sr, Cd, Pb, and As removal and pH profiles over time obtained using PW type I–V (Table 1). The profiles reveal two distinct patterns of toxic metals removal during the early stages of the batch reactions: the removal of Ba, Sr, and Cd increases while pH decreases, whereas the removal of Pb and As increases while pH increases. A decrease of pH for Ba, Sr, and Cd removal is attributed to precipitation of

Table 3
Toxic metals removal from PW types I-VII (Table 1).

	Type of produced water (PW)						
	I	II	III	IV	V	VI	VII
Final pH	7.08	7.38	7.31	7.32	7.45	7.61	7.26
Alkalinity increment (mg/L)	15.16	13.62	12.77	10.58	−22.34	−43.77	23.24
Ba removal (%)	2.05					3.61	2.1
Sr removal (%)		4.90				3.72	1.28
Cd removal (%)			17.29			15.16	8.19
Pb removal (%)				93.39		98.48	96.16
As removal (%)					4.75	12.57	17.73

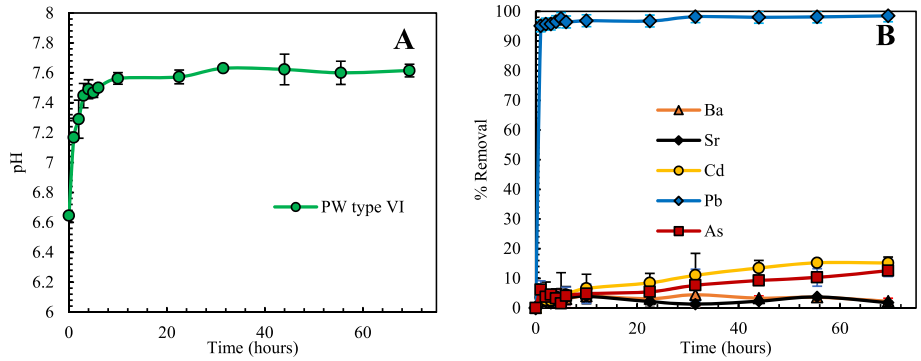

Fig. 2. Batch experimental results of mixed toxic metals removal by dolomite (PW type VI): A) pH profile; B) Toxic metals removal profile. PW type VI was supplied with $CaCO_3$ to increase the initial alkalinity (Table 1).

carbonate minerals according to: $BaCO_3 + H^+ \leftrightarrow Ba^{2+} + HCO_3^-$, for instance, where H^+ is produced along the carbonate mineral phase. Apparently, precipitation and sorption reactions of Ba, Sr, and Cd are faster than dolomite dissolution: $CaMg(CO_3)_2 + 2H^+ \leftrightarrow Ca^{2+} + Mg^{2+} + 2HCO_3^-$, when alkalinity is available (>10 mg/L) and pH is > 7.4. This is reflected by a decrease instead of an increase in pH. A rebound of Ba concentration in solution following the initial stages of the reaction is most due to an increase of Ca and Mg concentrations in solution from the dissolution of dolomite (Tables S3–S6). This behavior suggests that the removal of Ba, Sr, and Cd are mostly due to sorption reactions. Ca and Mg are known to compete for hydration sites of dolomite with metal cations such as Ba (Vilcáez, 2020). Likewise, an increase of pH for Pb and As removal during the early stages of the reaction is attributed to the dissolution of dolomite. Apparently, dolomite dissolution is faster than precipitation and sorption reactions of Pb and As, even if alkalinity is available when pH is < 7.4. This is reflected by the frequently reported increase of pH when water is exposed to dolomite.

Similar behavior of Ba (Fig. 1A) is observed with Sr (Fig. 1B), but the removal levels at equilibrium conditions are higher for Sr (5%) than for Ba (2%). Like with Ba and Sr, pH decreases with Cd removal from an alkaline pH to a close to neutral pH due to sorption and precipitation reactions (Fig. 1C). However, different from Ba and Sr whose removal are relatively small, the removal level of Cd at equilibrium conditions reaches 15% and the rebound of Cd concentration in solution after the initial stages of the reaction (when Cd removal is highest) is less pronounced than with Ba and Sr, suggesting that sorption reactions are more prominent for Cd than for Ba and Sr. If Cd precipitation reactions were more prominent than sorption reactions, lower alkalinity levels would have been observed with Cd than with Ba and Sr. Note that the initial and final alkalinity levels for Ba, Sr, and Cd as well as the final pH are practically the same (Table 3). Higher removal levels were attained for Pb (93.39%) (Fig. 1D) than for Ba (2%), Sr (5%), and Cd (15%). Different from the concentration profiles observed with Ba, Sr, and Cd where a fast decrease of their concentrations during the early stages of the reaction is followed up by a rebound of their concentrations in solution, the concentration of Pb in solution gradually decreased over time by 93.39%, and the initial pH, which was slightly acidic, increased gradually to ~7.4 (equilibrium pH) due the dissolution of dolomite. The net increase of alkalinity for Pb due to the dissolution of dolomite is smaller with Pb than with Ba, Sr, and Cd (Table 3). This behavior suggests that Pb removal is controlled by the dissolution of dolomite and that Pb precipitation as a carbonate mineral phase plays an important role.

Fig. 1E shows As removal and pH profiles over time obtained using PW type V (Table 1). The higher initial alkalinity for PW type V than for PW types I-IV was due to the formation of hydrochloric acid according to the following reaction: $AsCl_3 + 3H_2O \leftrightarrow As(OH)_3 + 3HCl$. The formed acid resulted in a pH of ~2 before adding $CaCO_3$. This acidic pH increased the dissolution of the supplied $CaCO_3$ resulting in a pH of 6.8 and an initial alkalinity of 58.2 mg/L. Alkalinity decreased instead of increasing despite the dissolution of dolomite. This behavior suggests that As removal under the tested conditions takes place through the precipitation of As as a carbonate mineral phase. However, the removal level does not exceed 5%, suggesting that Ca and/or Mg precipitation might be the dominant precipitation reaction sequestering As. Analogous behavior has been observed in groundwater systems as implied by previous studies (Alexandratos et al., 2007; Da'ana et al., 2021; Jensen, 2020; Lin et al., 2013; Tesoriero and Pankow, 1996).

To detect possible reaction interferences, we conducted experiments using synthetic PW type VI, which contained all tested toxic metals (Ba, Sr, Cd, Pb, and As). Fig. 2 shows their removal and pH profiles over time. The initial alkalinity of PW type VI was 98.86 mg/L (Table 1). With this alkalinity, removal of Pb from solution (85.64%) happened practically instantaneously, and the removal of As increased from 4.75% with an initial alkalinity of 58.2 mg/L (PW type V) to 12.57% with an initial alkalinity of 98.86 mg/L (PW type VI). The concentration profiles of the other toxic metals (Ba, Sr, and Cd) followed same patterns as when they were the only toxic metal present in solution (Fig. 1). These results support the hypothesis that precipitation reactions and thus alkalinity play an important role in the removal of toxic metals from PW, and that there are minor interferences between Ba, Sr, Cd, Pb, and As removal by dolomite at salinity and possible alkalinity levels of PW.

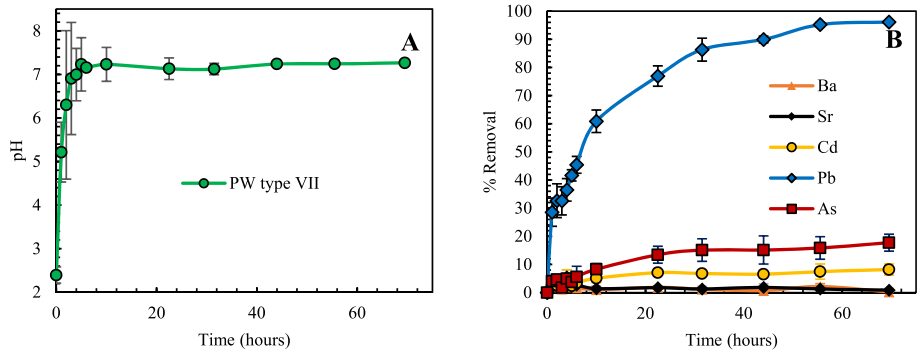

Fig. 3. Batch experimental results of mixed toxic metals removal by dolomite (PW type VII): A) pH profile; B) Toxic metals removal profile. PW type VII was not supplied with $CaCO_3$ to increase the initial alkalinity (Table 1.

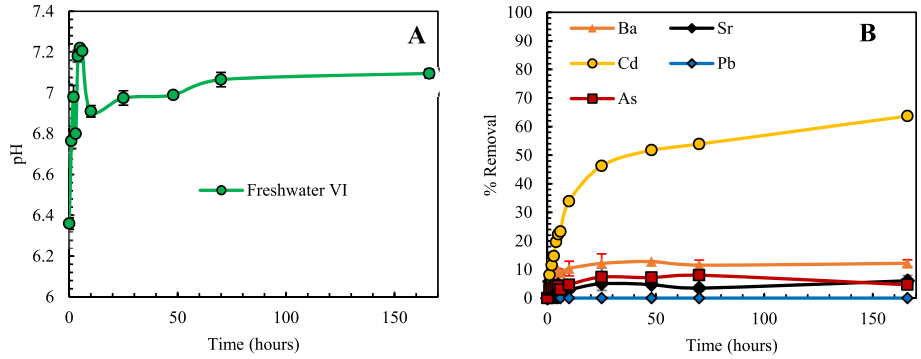

Fig. 4. Batch experimental results of mixed toxic metals removal by dolomite (FW type VI): A) pH profile; B) Toxic metals removal profile. FW type VI was supplied with $CaCO_3$ to increase the initial alkalinity (Table 2).

Table 4
Toxic metals removal from FW types I-VII (Table 2).

	Types of produced water (FW)						
	I	II	III	IV	V	VI	VII
Final pH	7.58	7.96	7.05	7.83	8.06	7.1	6.83
Alkalinity increment (mg/L)	47.80	43.90	3.90	42.20	43.80	−4.00	8.20
Ba removal (%)	22.02					12.19	5.54
Sr removal (%)		8.94				6.08	2.06
Cd removal (%)			68.20			63.68	38.29
Pb removal (%)				99.78		0.00	99.48
As removal (%)					5.48	4.68	15.07

To confirm that the addition of $CaCO_3$ to increase alkalinity played a role in the observed removals of Ba, Sr, Cd, Pb, and As, we conducted experiments using synthetic PW type VII, which was not supplied with $CaCO_3$. Fig. 3 shows Ba, Sr, Cd, Pb, and As removal and pH profiles over time obtained using PW type VII (Table 1). The initial pH was acidic due to the formation of hydrochloric acid by $AsCl_3$. Different from the removal profiles obtained with PW type VI (Fig. 2) where Pb removal happened practically instantaneously, Pb removal with PW type VII happened gradually. Slow removal rates of Pb support the hypothesis that precipitation of Pb and possibly As as carbonate minerals contribute to the removal of Pb and As from PW more than it does to the removal of Ba, Sr, and Cd. Moreover, these results indicate that under low alkalinity conditions, the precipitation of toxic metals as carbonate minerals relies on alkalinity generated from the dissolution of dolomite.

To elucidate a possible different response of toxic metals to alkalinity and dolomite dissolution at FW salinity levels, we conducted

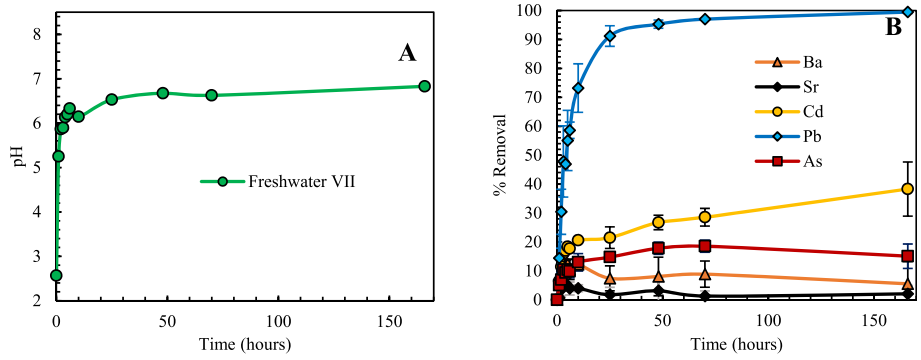

Fig. 5. Batch experimental results of mixed toxic metals removal by dolomite (FW type VII): A) pH profile; B) Toxic metals removal profile. FW type VII was not supplied with $CaCO_3$ to increase the initial alkalinity (Table 2).

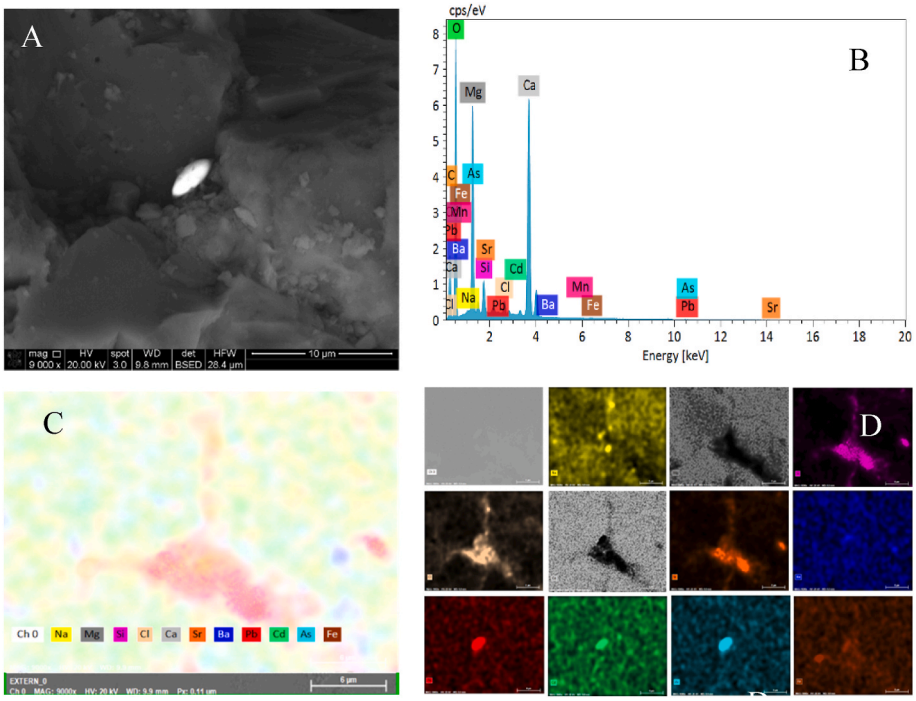

Fig. 6. SEM-EDS mapping of dolomite grain surface after 72 h of batch reaction using PW type VI (Ba, Sr, Cd, Pb, and As): A) SEM micrograph showing toxic metals carbonate phase with oval shape in the center, B) X-ray spectrum showing the elemental composition of the bulk samples, C) EDS mapping, and D) EDS mapping layers for single metals.

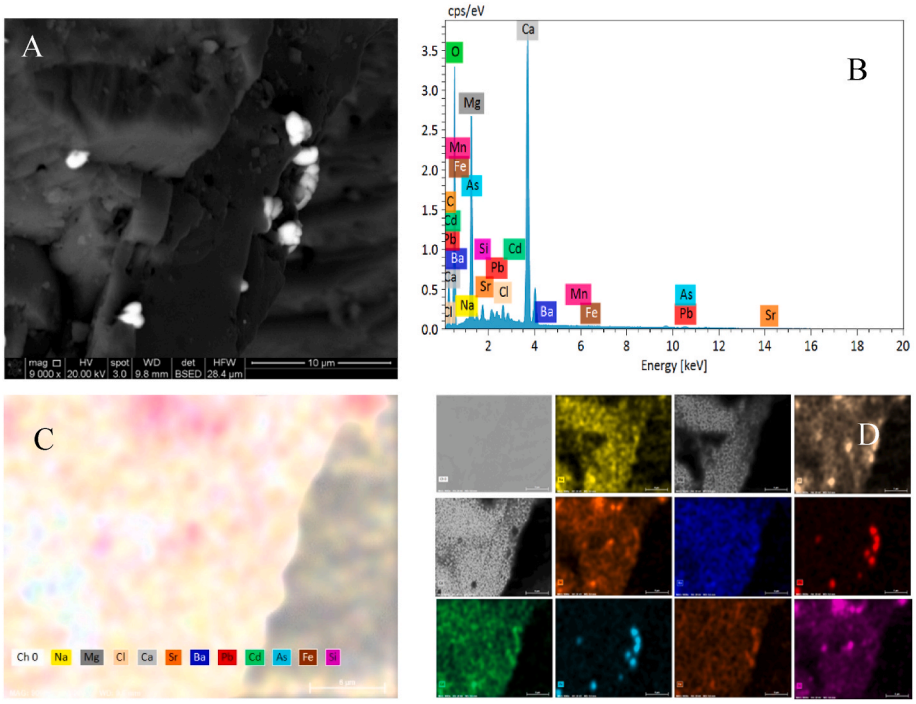

Fig. 7. SEM-EDS mapping of dolomite grain surface after 72 h of batch reaction using PW type VII (Ba, Sr, Cd, Pb, and As): A) SEM micrograph showing toxic metals carbonate phase at the edges of the dolomite grain, B) X-ray spectrum showing the elemental composition of the bulk samples, C) EDS mapping, and D) EDS mapping layers for single metals.

experiments using synthetic FW containing single (FW types I–V) and mixed (FW types VI and VII) toxic metals (Table 2). In accordance with previous studies showing that salinity (NaCl) inhibits sorption reactions, higher removal levels were obtained with FW for Ba (22.02%), Sr (8.94%), Cd (68.2%), Pb (99.78%), and As (5.48%) (Fig. S2 and Table 3). However, despite the same initial concentrations of toxic metals in solution, Ba removal increases ten times while Sr removal only increases two times by reducing salinity (NaCl) from to 40 g-NaCl/L (PW) to 0.1 g-NaCl/L (FW). Moreover, interestingly As removal is practically the same with PW and FW. The results highlight the different

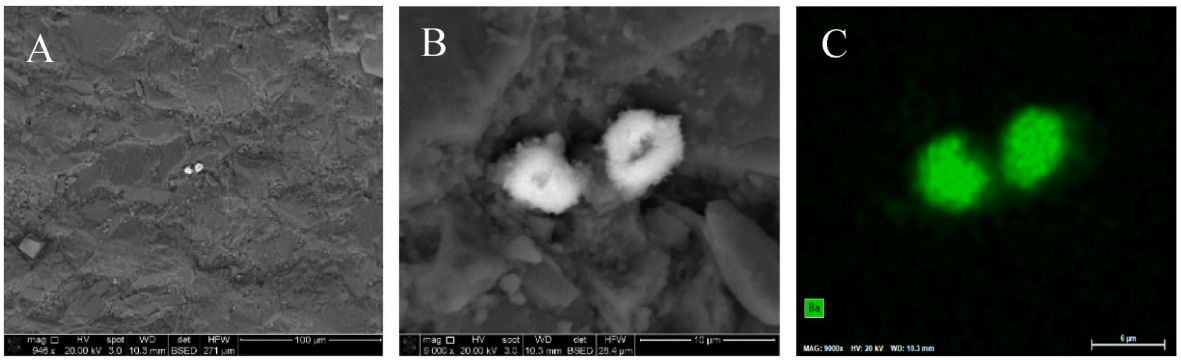

Fig. 8. SEM-EDS analysis of dolomite grain surface after 72 h of batch reaction using PW type I (Ba): A) SEM shows Ba precipitates in the middle of the picture as light-colored grains, B) Zoom-in of A, showing Ba precipitate, and C) SEM-EDS mapping of B showing Ba precipitate in green color.

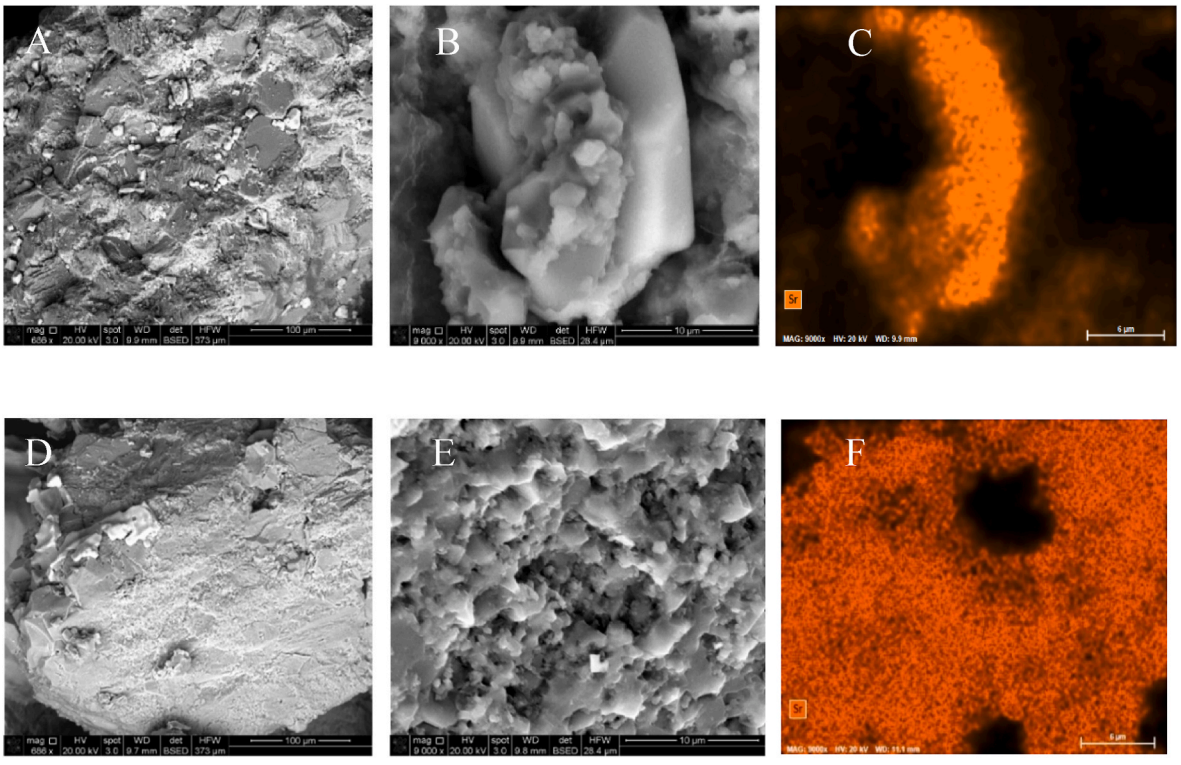

Fig. 9. SEM-EDS analysis of dolomite grain surface after 72 h of batch reaction using PW type II (Sr): A) SEM shows Sr and NaCl precipitates (light gray), B) Zoom-in of A showing a precipitate, C) EDS mapping of B showing that the precipitate contains Sr, D) SEM of high silica dolomite grain showing NaCl on the upper left side of the image, E) Zoom-in of D showing amorphous silica, and F) SEM-EDS mapping of E showing Sr a sorbed phase on the high silica dolomite grain in orange color.

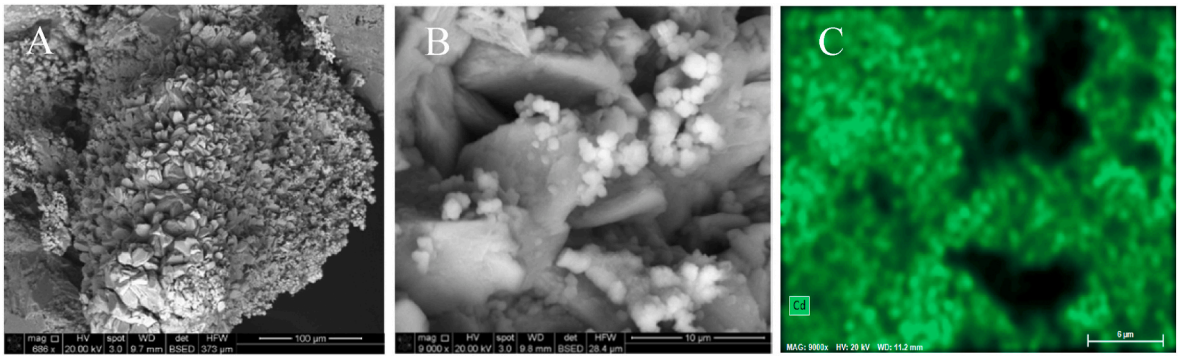

Fig. 10. SEM-EDS analysis of dolomite grain surface after 72 h of batch reaction using PW type III (Cd): A) SEM shows a high Fe dolomite grain, B) Zoom-in of A showing a cluster-shaped phase of Fe (light color), C) EDS mapping of B showing Cd sorption on dolomite.

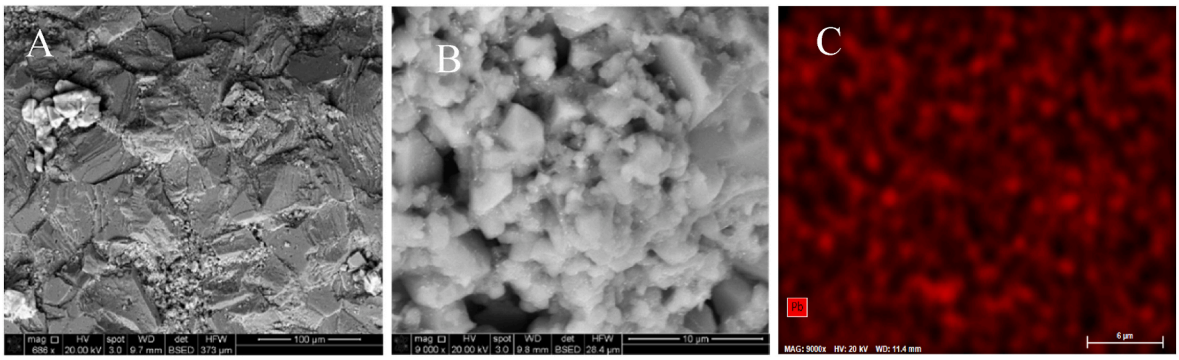

Fig. 11. SEM-EDS analysis of dolomite grain surface after 72 h of batch reaction using PW type IV (Pb): A SEM image showing NaCl grain (light gray) precipitated on the dolomite surface, B) Zoom-in of A showing nanoscale Pb precipitates of white color on dolomite grain/crystal edges, C) EDS mapping of B showing Pb precipitates on dolomite.

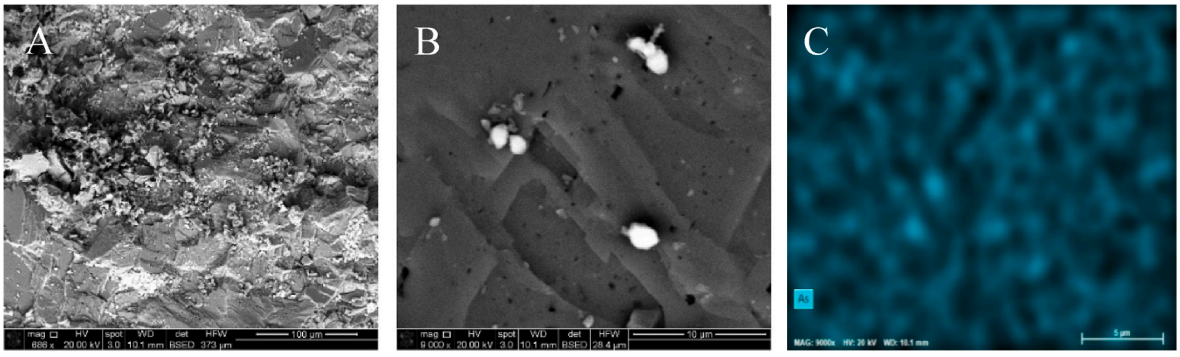

Fig. 12. SEM-EDS analysis of dolomite grain surface after 72 h of batch reaction using PW type V (As): A) SEM image showing a lot of debris, B) Zoom-in of A showing As precipitate of different in bright color on the dolomite crystal face, C) EDS mapping of B showing As as precipitates.

behavior of toxic metals in FW and PW. The inhibitory effect of salinity on sorption reactions is different depending on the type of toxic metal and initial alkalinity. Ba, Sr, and Cd removal decreases 10, 2, and 4 times by increasing salinity (NaCl) from to 0.1 g-NaCl/L (PW) to 40 g-NaCl/L (FW), while As removal is practically the same regardless of salinity.

Fig. 4 shows Ba, Sr, Cd, Pb, and As removal and pH profiles over time obtained using FW type VI that had an initial alkalinity of 15.29 mg/L. Different from PW type VI, which was also added with $CaCO_3$ to increase alkalinity, Pb solubility was practically zero with FW type VI, highlighting the different solubility of toxic metals in PW and FW. Similar removal levels (Table 4) obtained using single (FW type 1-V) and mixture toxic metals (FW type VI) confirms that their removals do not interfere with each other in both FW and PW.

To confirm the role of alkalinity in toxic metals precipitation from FW, we conducted batch experiments using FW type VII that was not added with $CaCO_3$ to increase alkalinity. In accordance with our hypothesis regarding the role of alkalinity, Pb did not precipitate immediately as it did with FW type VI. Its removal rate was slow as dolomite dissolution provided the required alkalinity for Pb precipitation. This is reflected by a concomitant increase of pH and removal of Pb (Fig. 5). Most importantly, lower removal levels of Ba, Sr, and Cd were obtained with FW type VII than with FW type VI. This confirms that the removal of Ba, Sr, and Cd by sorption reactions decreases with decreasing pH, and that alkalinity promotes the removal of not only Pb and As, but also Ba, Sr, and Cd as carbonate minerals. However, it is noteworthy that Ba, Sr, and Cd removal is mostly due to sorption reactions. An increase of Ba, Sr, and Cd removal by precipitation reactions, due to the availability of alkalinity, does not surpass Ba, Sr, and Cd removal by sorption reactions.

Table S7 shows the measured concentrations of toxic metals in PW types VI and VII, as well as in FW types VI and VII after months without dolomite in solution. Practically the same concentrations of toxic metals without dolomite in solution confirm the that observed decrease of toxic metals concentrations in the conducted batch reaction experiments were due to the presence of dolomite in solution. The 2.8% average total difference in the measured concentrations can be attributed to operator or instrument error.

4.2. SEM-EDS analysis

To verify the precipitation of toxic metals, we used SEM-EDS analysis to examine changes in the morphology and elemental composition of dolomite grains collected from the batch reactors after 72 h of reaction. Fig. S3 shows SEM images of dolomite grains collected from the batch experiments conducted using PW type I–V.

Figs. 6 and 7 show SEM-EDS images of the dolomite surface at the end of the experiments conducted using synthetic PW types VI (with added alkalinity) and VII (without added alkalinity). The analysis confirms the sorption of all tested toxic metals on dolomite. However, and more importantly, in accordance with the concentration profiles of Pb and As, SEM-EDS analysis results confirm that their precipitation as carbonates plays a prominent role in the removal of toxic metals such us Pb and As by dolomite. The SEM-EDS images show that the bright white spots in the SEM images contain Pb and/or As.

Figs. 8–12 show SEM-EDS images of the dolomite surface at the end of the experiments conducted using synthetic PW types I–V which contained single toxic metals.

Ba precipitates were scarce and found only in cavities on the dolomite surface or between dolomite crystals (Fig. 8). The detected Ba precipitates were characterized by having rough surfaces, irregular shapes, and different sizes (2–10 μm). According to literature (Tesoriero and Pankow, 1996), Ba in nature can precipitate as witherite ($BaCO_3$) (Antao and Hassan, 2009), coprecipitate with carbonate minerals such

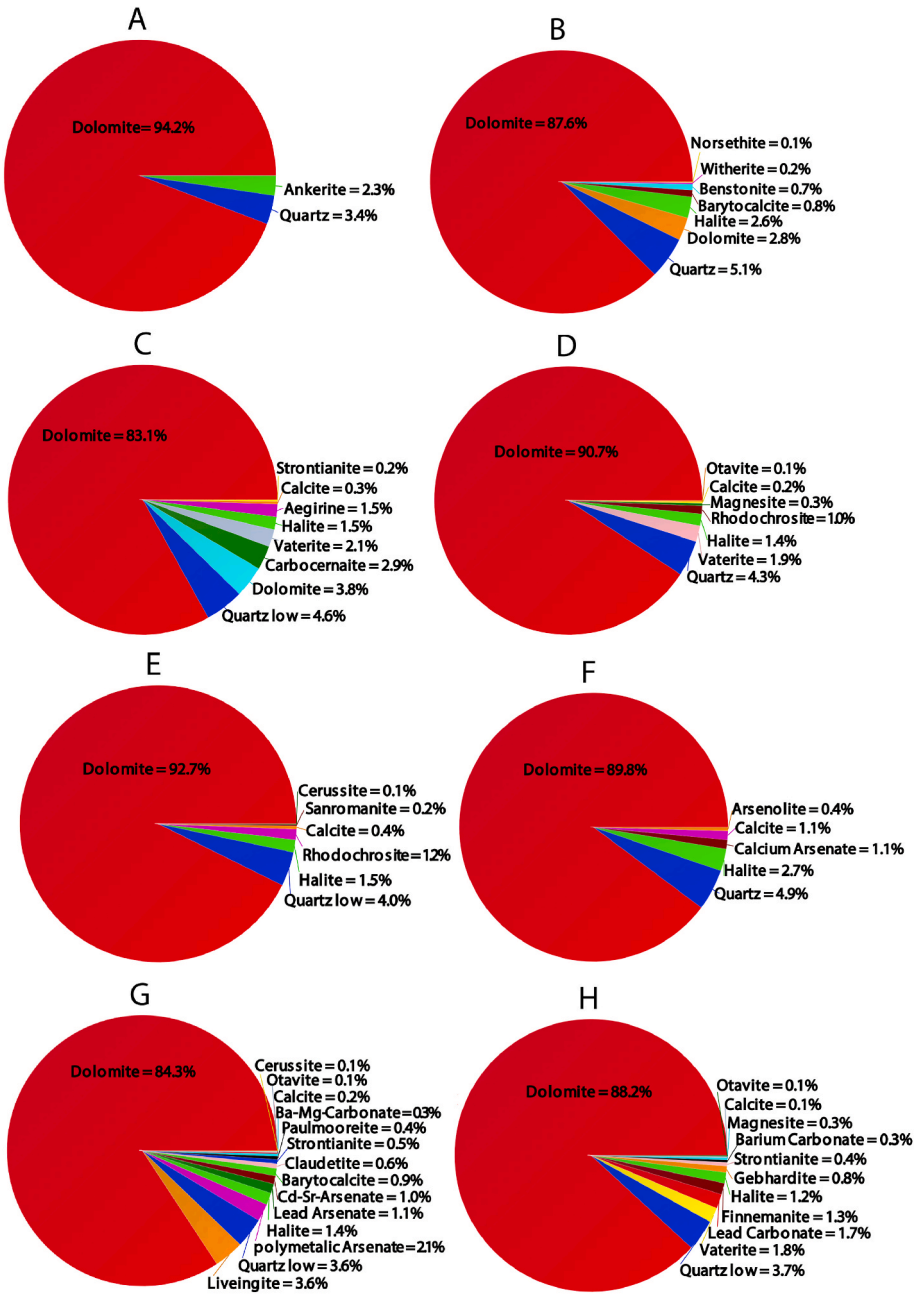

Fig. 13. Semiquantitative analyses from high-resolution XRD (Fig. S9) conducted on the powdered dolomite samples collected from batch reaction experiments: A) Control sample, B) PW type I (Ba), C) PW type II (Sr), D) PW type III (Cd), E) PW type IV (Pb), F) PW type V (As), G) PW type VI (Ba, Sr, Cd, Pb, and As), and H) PW VII (Ba, Sr, Cd, Pb, and As).

as calcite, and/or it can form hydrated amorphous carbonate phases. In our experiments, Ba precipitates were found along with NaCl precipitates (Figs. S4 and S5).

Sr was also found on the dolomite surface as precipitate and sorbed species (Fig. 9). However, like Ba, Sr precipitates were scarce and characterized by angular surfaces, larger size (~20 μm long), and they were found along with NaCl precipitates. Interestingly, Sr mainly sorbed on quartz (SiO_2) which is a minor component of Arbuckle dolomite (Fig. S6). This observation suggests that Sr has a higher affinity for quartz than for dolomite.

Cd was hardly found as a precipitate in our batch reaction experiments for single toxic metals. Cd was only detected as sorbed phase on ferric dolomite grains (Fig. 10 and Fig. S7), indicating that the high removal of Cd (17.29%) was mostly due to sorption reactions. Conversely, Pb removal was controlled mainly by precipitation reactions. Pb was commonly found as a precipitate on the dints or inside edges of dolomite grains/crystals (Fig. 11 and Fig. S8). Pb precipitates are characterized by nanoscale oval shape precipitates.

As was found as 1–3 μm size precipitates with irregular shapes on dolomite (Fig. 10). Different from the other toxic metals, As precipitated directly on the crystal face of dolomite, and it was detected as precipitate and sorbed phases (Fig. 12 and Fig. S9). In this study, precipitate and sorbed phases are identified by contrasting SEM images showing precipitates and the corresponding EDS map of elements that indicate the elemental composition of the imaged precipitates. For instance, if the EDS map shows an element occurring in locations where precipitates are seen on the SEM image as well as on the rest of the analyzed dolomite surface, we conclude that this metal is removed by both precipitation and sorption reactions.

Table 5
Aqueous phase equilibrium complexation reactions.

Reaction	Log K_{eq} (25 °C)
$OH^- + H^+ \leftrightarrow H_2O$	13.991
$CO_2(aq) + H_2O \leftrightarrow H^+ + HCO_3^-$	−6.342
$CO_3^{2-} + H^+ \leftrightarrow HCO_3^-$	10.325
$CaOH^+ + H^+ \leftrightarrow Ca^{2+} + H_2O$	12.852
$SrOH^+ + H^+ \leftrightarrow Sr^{2+} + H_2O$	13.290
$CdOH^+ + H^+ \leftrightarrow Cd^{2+} + H_2O$	10.075
$PbOH^+ + H^+ \leftrightarrow Pb^{2+} + H_2O$	7.695
$CaCO_3(aq) + H^+ \leftrightarrow Ca^{2+} + HCO_3^-$	7.009
$MgCO_3(aq) + H^+ \leftrightarrow HCO_3^- + Mg^{2+}$	7.356
$SrCO_3(aq) + H^+ \leftrightarrow Sr^{2+} + HCO_3^-$	7.470
$CdCO_3(aq) + H^+ \leftrightarrow Cd^{2+} + HCO_3^-$	7.328
$PbCO_3(aq) + H^+ \leftrightarrow Pb^{2+} + HCO_3^-$	3.748
$CaCl^+ \leftrightarrow Ca^{2+} + 2Cl^-$	0.701
$MgCl^+ \leftrightarrow Mg^{2+} + Cl^-$	0.139
$SrCl^+ \leftrightarrow Sr^{2+} + Cl^-$	0.253
$CdCl^+ \leftrightarrow Cd^{2+} + Cl^-$	−2.706
$PbCl^+ \leftrightarrow Pb^{2+} + Cl^-$	−1.432
$CO_2(g) + H_2O \leftrightarrow H^+ + HCO_3^-$	−7.809

Table 6
Mineral phase reactions.

Carbonate	Reaction	Log K_{eq} (25 °C)
Dolomite	$CaMg(CO_3)_2 + 2H^+ \leftrightarrow Ca^{2+} + Mg^{2+} + 2HCO_3^-$	−0.7717
Calcite	$CaCO_3 + H^+ \leftrightarrow Ca^{2+} + HCO_3^-$	−0.8070
Magnesite	$MgCO_3 + H^+ \leftrightarrow Mg^{2+} + HCO_3^-$	−1.5934
Strontionite	$SrCO_3 + H^+ \leftrightarrow Sr^{2+} + HCO_3^-$	−0.7702
Otavite	$CdCO_3 + H^+ \leftrightarrow Cd^{2+} + HCO_3^-$	−1.2378
Cerussite	$PbCO_3 + H^+ \leftrightarrow Pb^{2+} + HCO_3^-$	1.0681

4.3. XRD analysis

To elucidate whether the observed precipitates were crystalized carbonates, we conducted high-resolution XRD analyses. Fig. 13 shows all the minerals detected through semiquantitative analysis of obtained high-resolution XRD spectra Analysis was done on a control dolomite sample (Fig. 13A) collected before conducting the batch experiment as well as on samples collected after conducting each batch experiment (Fig. 13B–H).

The obtained XRD spectra (Fig. S10) display major (>5%), minor (<5%), and even trace (<1%) minerals in the analyzed samples. The major mineral in the control sample was dolomite. However, XRD spectra showed minor content of silica (quartz) and carbonate (ankerite) minerals in some control samples (e.g., Fig. 13A). The origin of the detected silica minerals could be either from terrigenous siliciclastic sand grains entered by different transportation mechanisms such as wind into the precursor carbonate depositional settings, or from amorphous biogenic silica crystallization driven by complex hydrothermal diagenetic processes that Arbuckle Group had undergone (Bettermann and Liebau, 1975; Temple et al., 2020). Carbonate minerals such as calcite and vaterite were only found in samples collected after conducting batch reaction experiments, confirming that these minerals were precipitated during the experiments. Evaporate minerals (e.g., halite) were also detected in all samples collected at the end of the experiments but not in the control samples, suggesting that halite precipitated during the experiments or during the drying of samples for XRD analysis. Remarkably, based on XRD semiquantitative analysis (Fig. 13), the total mass fraction of precipitates is 10–17% of dolomite mass after 72 h of reaction when equilibrium is reached, and the detected minerals are significantly diverse from sample to sample. At first glance, this might be expected because we used natural dolomite rocks. Traces of minerals might be slightly different from sample to sample even for the same rock. However, with more careful examination, we recognized that the chemistry of these trace of minerals corresponds to the chemical composition of the employed type of PW. For example, the carbonate minerals phases detected for samples collected from experiments conducted using PW type I–V are witherite ($BaCO_3$), strontianite ($SrCO_3$), otavite ($CdCO_3$), cerussite ($PbCO_3$), and calcium arsenate ($Ca_3(AsO_4)_2$) (Fig. 13B–F), which are known to be more thermodynamically feasible at standard conditions (Antao and Hassan, 2009; Anthony et al., 1995). In addition to these minerals, several other carbonate and oxide phases were also detected. For instance, As oxides were found in the samples collected from experiments conducted using PW type V (Fig. 13F). This was probably due to the high tendency of As to form oxide phases in the aqueous environments (Neuberger and Helz, 2005). Although the employed synthetic PW did not contain sulfur, Fig. 13G shows the formation of liveingite ($Pb_9As_{12}S_{28}$). This is attributed to sulfur mineral impurities we detected in some dolomite grains analyzed by XRD. Like sulfate minerals, dolomite can be an evaporite mineral. Depending on the dolomite depositional environment, sulfate minerals such as gypsum and anhydrite can occur associated with dolomite, especially with dolomite of evaporative origin. Consequently, minor or trace amounts of sulfur in solution was possible from dolomite dissolution.

XRD analysis on samples collected from experiments using PW types VI and VII which contained mixture toxic metals, show very complex polymetallic minerals. Different from the results obtained using PW types I–V which contained single toxic metals, detected phases were coprecipitated arsenate minerals such as strontium cadmium arsenate ($SrCd(As_2O_7)$) and lead arsenate ($PbAs_2O_4$) (Fig. 13G&H). These minerals have been found in dolomite of low hydrothermal origin (Anthony et al., 1995).

5. Geochemical modeling

Measuring the exact amount of toxic metal removed from PW by sorption and precipitation reactions presents several challenges and it requires additional analytical methods. To confirm the thermodynamic feasibility and to determine the possible extent of precipitation reactions under the tested PW compositions, here we simulate the conducted experiments using CrunchFlow geochemical modeling software (Steefel and Lasaga, 1994). CrunchFlow incorporates the EQ3/EQ6 thermodynamic database (Wolery et al., 1990). Due to the unavailability of thermodynamic data for Ba and As carbonate minerals precipitation reactions, simulations are done for synthetic PW type VI containing only Sr, Cd, and Pb.

Tables 5 and 6 show the aqueous phase complexation and carbonate precipitation reactions along with corresponding equilibrium constants we used for simulations. Details on the employed sorption complexation model can be found in Ebrahimi and Vilcáez (2018a). Briefly, the model accounts for the three types of hydration sites of dolomite (>$CaOH^o$, >$MgOH^o$, and >CO_3H^o). An intrinsic stability constant (K_{int}) determines the concentration of divalent cations on the surface of dolomite:

$$K_{int} = \frac{[> CO_3Me^+][H^+]}{[> CO_3H^o][Me^{2+}]} \quad (1)$$

where Me is Ca, Mg, Sr, Cd, or Pb. Employed log values of K_{int} for these metals are −1.8, −2.0, −4.66, −0.233, and −2.33, respectively. K_{int} for Ca and Mg corresponds to measured values at low salinity conditions (Pokrovsky et al., 1999), whereas K_{int} for Sr, Cd, and Pb are assumed values based on observed removal levels.

Except for dolomite, precipitation/dissolution reactions of carbonate minerals (Table 5) are assumed to be equilibrium (instantaneous) reactions. Dissolution/precipitation reactions of dolomite are kinetic reactions represented by the transition state theory (TST) model (Lasaga, 1984):

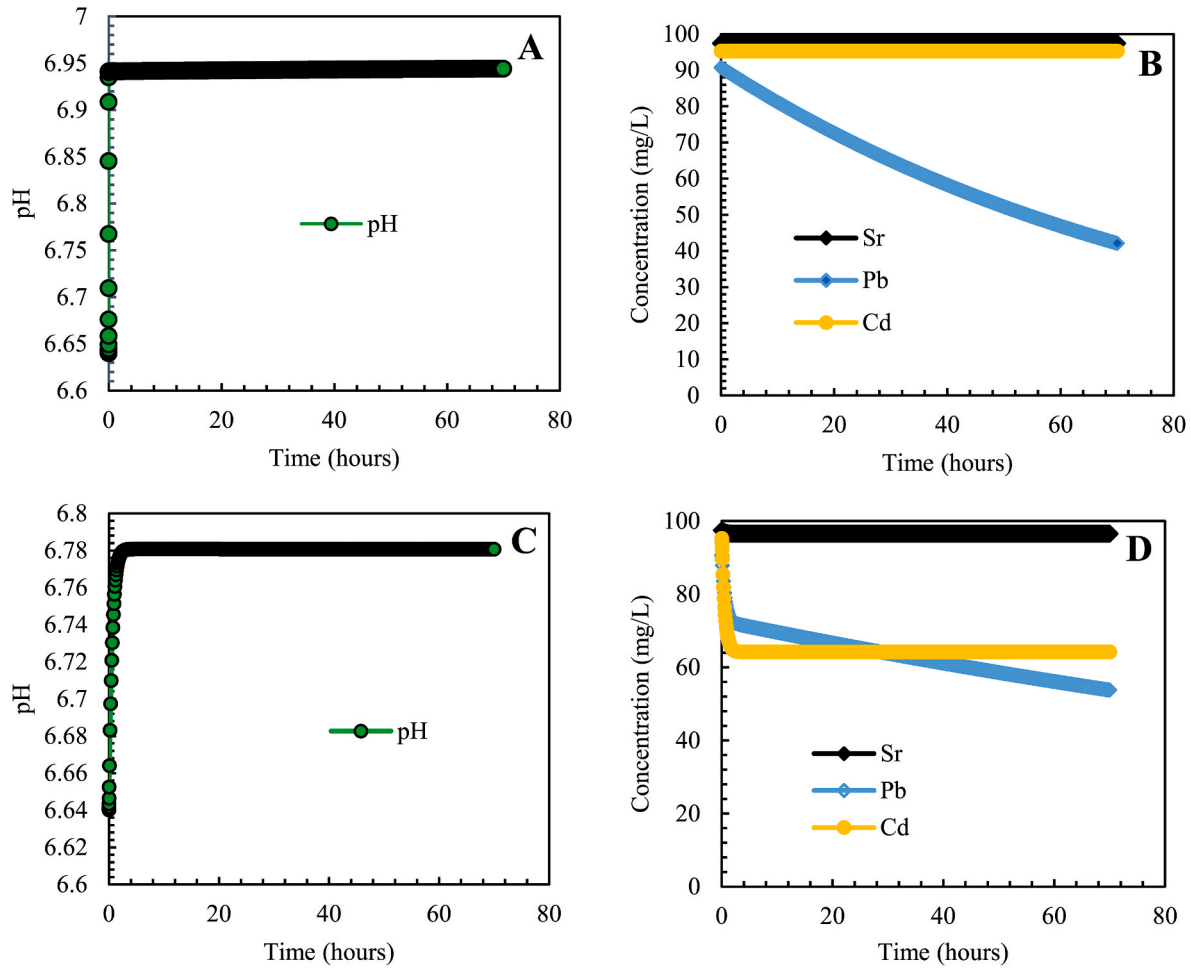

Fig. 14. Simulated pH variations and concentration profiles of selected toxic metals: Top (A&B)– Accounting only for precipitation reactions. Bottom (C&D)– Accounting for both sorption and precipitation reactions. PW composition corresponds to PW type VI (Table 1).

$$-R_{Dolomite} = Ak_m[H^+]\left\{1 - \frac{[HCO_3^-]^2[Ca^{2+}][Mg^{2+}]}{[H^+]K_{eq}}\right\} \quad (2)$$

where k_m is the intrinsic rate constant, K_{eq} is the equilibrium constant of dolomite dissolution/precipitation (Table 6), and A is the surface area of dolomite. k_m and K_{eq} values included in the widely employed EQ (2)/EQ6 database are used for simulations. Other parameter values for dolomite including references can be found in (Ebrahimi and Vilcáez, 2018a).

Fig. 14 (A&B) shows concentration profiles of Sr, Cd, and Pb simulated assuming only precipitation/dissolution reactions are possible. The simulation results indicate that without sorption reactions, concentrations of Sr and Cd in PW type VI should have remained practically constant because precipitation of strontianite and otavite are not thermodynamically favored. Only the concentration of Pb should have decreased since its precipitation as cerussite is thermodynamically favored. This simulation results confirm that sorption is the main reaction type controlling the removal of Ba, Sr, and Cd by dolomite and that indeed the amount of strontianite and otavite that precipitates on dolomite is negligible as shown by the SEM-EDS analyses conducted in this study. Fig. 14 (C&D) shows concentration profiles of Sr, Cd, and Pb simulated accounting for the possibility of precipitation/dissolution and sorption reactions. Interestingly, the concentration profiles resemble measured removal levels of Sr, Cd, and Pb. However, the simulated removal level for Pb is not as high as the measured one. These simulation results confirm the precipitation and coprecipitation of Pb as complex carbonate minerals. Their formation needs to be included in the model to reproduce experimental results. pH in both cases increases and is in accordance with measured values confirming that pH and thus alkalinity is a function of the reactivity of dolomite. Note that the model captures the dependency of cerussite precipitation on dolomite dissolution.

6. Conclusions

Batch reaction experiments were conducted to assess the role of alkalinity and dolomite dissolution on the removal of high concentrations (~100 mg/L) of single and mixture toxic metals (Ba, Sr, Cd, Pb, and As) from PW (TDS >68,000 mg/L) and FW (TDS <2000 mg/L) by dolomite. Ba, Sr, Cd, Pb, and As undergo sorption and precipitation reactions. However, the degree and therefore relevance of both reactions at salinity and alkalinity levels of PW are different depending on the type of toxic metal. Ba, Sr, and Cd mostly undergo sorption reactions, whereas Pb and As undergo both sorption and precipitation reactions. Alkalinity promotes the removal of Ba, Sr, and Cd through sorption reactions by reducing the concentration of H^+ which competes for hydration (sorption) sites of dolomite, whereas alkalinity (CO_3^{2-} and HCO_3^-) promotes the removal of Pb and As by forming carbonate minerals. Given the role of alkalinity in the removal of Ba, Sr, Cd, Pb and As by sorption and precipitation reactions, dolomite dissolution plays an important role in the removal of toxic metals from PW. This is particularly the case of Pb whose removal rate is proportional to the dissolution rate of dolomite. These conclusions are supported by SEM-EDS mapping results showing different ratios of sorbed and precipitated phases of Ba, Sr, Cd, Pb, and As on dolomite grains, as well as by XRD analysis

showing different amounts of Ba, Sr, Cd, and Pb precipitates as carbonate minerals (e.g., witherite, strontionite, otavite, and cerussite), As as oxide (calcium arsenate), and several other minerals phases with complex composition, such as strontium cadmium arsenate (SrCd(As_2O_7)) and lead arsenate ($PbAs_2O_4$). Ba precipitates in cavities or between dolomite crystals, Sr on quartz in dolomite, Cd on ferric dolomite grains, Pb on the dints or inside edges of dolomite grains, and As precipitates directly on the surface of dolomite. Simulations accounting for complexation reactions in the aqueous and mineral phases, equilibrium precipitation reactions of carbonate minerals, and kinetic dissolution/precipitation reaction of dolomite, confirm the thermodynamic feasibility of small amounts of Sr, and Cd precipitation and much larger precipitation amounts of Pb as carbonate minerals. Comparison between attained removal levels of Ba, Sr, Cd, Pb, and As from PW and FW of the same alkalinity shows that the effect of salinity is very different depending on the type of toxic metal. Salinity inhibits sorption reactions of Ba, Sr, and Cd and it promotes the solubility of Pb, but it does not seem to affect the removal of As by dolomite. The findings of this study have large practical implications to predict the fate and transport of toxic metals in dolomite saline aquifers injected with PW and to design optimum operational conditions to remove toxic metals from PW by dolomite filtration.

Funding

This work was supported by the National Science Foundation under Grant CBET-220036.

Declaration of competing interest

The authors declare that they have no known competing financial interests or personal relationships that could have appeared to influence the work reported in this paper.

Data availability

No data was used for the research described in the article.

Acknowledgments

This is Oklahoma State University Boone Pickens School of Geology contribution number 2023–139.

Appendix A. Supplementary data

Supplementary data to this article can be found online at https://doi.org/10.1016/j.apgeochem.2023.105879.

References

Alexandratos, V.G., Elzinga, E.J., Reeder, R.J., 2007. Arsenate uptake by calcite: macroscopic and spectroscopic characterization of adsorption and incorporation mechanisms. Geochem. Cosmochim. Acta 71 (17), 4172–4187.
Alley, B., Beebe, A., Rodgers Jr., J., Castle, J.W., 2011. Chemical and physical characterization of produced waters from conventional and unconventional fossil fuel resources. Chemosphere 85 (1), 74–82.
Antao, S.M., Hassan, I., 2009. The orthorhombic structure of CaCO3, SrCO3, PbCO3 and BaCO3: linear structural trends. Can. Mineral. 47 (5), 1245–1255.
Anthony, J.W., Bideaux, R.A., Bladh, K.W., Nichols, E., Monte, C., 1995. Handbook of Mineralogy. Mineralogical Society of America, USA. Chantilly, VA 20151-1110.
Anthony, J.W., Bideaux, R.A., Bladh, K.W., Nichols, M.C., 2007. Borates, carbonates, sulfates. In: Handbook of Mineralogy. Mineralogical Society of America, V.
Balci, N., Demirel, C., Ön, S.A., Gültekin, A.H., Kurt, M.A., 2018. Evaluating abiotic and microbial factors on carbonate precipitation in Lake Acigöl, a hypersaline lake in Southwestern Turkey. Quat. Int. 486, 116–128.
Ballinger, D.G., 1979. Methods for chemical analysis of water and wastes, 1979. In: United States Environmental Protection Agency. EPA 600/4-79-020. Environmental Monitoring and Support Labotatory Cincinnati, Ohio, 353.2-1 to 353.2-5 (nitrate analysis) and 325.2-1 to 325.2-2 (chloride analysis).
Bettermann, P., Liebau, F., 1975. The transformation of amorphous silica to crystalline silica under hydrothermal conditions. Contrib. Mineral. Petrol. 53 (1), 25–36.
Brown, J.G.E., Parks, G.A., 2001. Sorption of trace elements on mineral surfaces: modern perspectives from spectroscopic studies, and comments on sorption in the marine environment. Int. Geol. Rev. 43 (11), 963–1073.
Chen, X., et al., 2021. Microbially induced carbonate precipitation techniques for the remediation of heavy metal and trace element–polluted soils and water. Water, Air, Soil Pollut. 232 (7), 1–15.
Da'ana, D.A., et al., 2021. Removal of toxic elements and microbial contaminants from groundwater using low-cost treatment options. Current Pollution Reports 7 (3), 300–324.
Dixit, S., Hering, J.G., 2003. Comparison of arsenic (V) and arsenic (III) sorption onto iron oxide minerals: implications for arsenic mobility. Environ. Sci. Technol. 37 (18), 4182–4189.
Drever, J.I., 1997. The Geochemistry of Natural Waters: Surface and Groundwater Environments, vol. 436, pp. p87–p105.
Ebrahimi, P., Borrok, D.M., 2020. Mobility of Ba, Sr, Se and as under simulated conditions of produced water injection in dolomite. Appl. Geochem. 118, 104640.
Ebrahimi, P., Vilcáez, J., 2018a. Effect of brine salinity and guar gum on the transport of barium through dolomite rocks: implications for unconventional oil and gas wastewater disposal. J. Environ. Manag. 214, 370–378.
Ebrahimi, P., Vilcáez, J., 2018b. Petroleum produced water disposal: mobility and transport of barium in sandstone and dolomite rocks. Sci. Total Environ. 634, 1054–1063.
Ebrahimi, P., Vilcáez, J., 2019. Transport of barium in fractured dolomite and sandstone saline aquifers. Sci. Total Environ. 647, 323–333.
Emmons, R.V., et al., 2022. Unraveling the complex composition of produced water by specialized extraction methodologies. Environ. Sci. Technol. 56 (4), 2334–2344.
Ezennubia, V., Vilcáez, J., 2023. Removal of oil hydrocarbons from petroleum produced water by indigenous oil degrading microbial communities. JWPE 51, 103400. https://doi.org/10.1016/j.jwpe.2022.103400.
Federation, W.E., Aph Association, 2005. Standard Methods for the Examination of Water and Wastewater, 21th Edition. American Public Health Association (APHA), Washington, DC, USA. 4-75 to 4-76 (chloride method 4500-Cl G) and 4-127 to 4-129 (nitrate method 4500-NO3 I).
Fukushi, K., Munemoto, T., Sakai, M., Yagi, S., 2011. Monohydrocalcite: a promising remediation material for hazardous anions. Sci. Technol. Adv. Mater. 12 (6), 064702.
Guerra, K., Dahm, K., Dundorf, S., 2011. Oil and Gas Produced Water Management and Beneficial Use in the Western United States. US Department of the Interior, p. 157.
Holail, H., Al-Hajari, S., 1997. Evidence of an Authigenic Origin for the Palygorskite in a Middle Eocene Carbonate Sequence from North Qatar, vol. 17. Qatar Univ. Sci. J., pp. 405–418
Ingles, M., Anadon, P., 1991. Relationship of clay minerals to depositional environment in the non-marine eocene pontils Group, SE ebro basin (Spain). J. Sediment. Petrol. 61, 926–939.
Jensen, J., 2020. The Role of Carbonate Minerals in Arsenic Mobility in a Shallow Aquifer Influenced by a Seasonally Fluctuating Groundwater Table. Masters thesis, Utah State University.
Kaasa, B., Østvold, T., 1996. Alkalinity in Oil Field Waters-What Alkalinity Is and How it Is Measured.
Kim, Y., Kwon, S., Roh, Y., 2021. Effect of divalent cations (Cu, Zn, Pb, Cd, and Sr) on microbially induced calcium carbonate precipitation and mineralogical properties. Front. Microbiol. 12, 646748.
Kumari, D., et al., 2016. Microbially-induced carbonate precipitation for immobilization of toxic metals. Adv. Appl. Microbiol. 94, 79–108.
Lasaga, A.C., 1984. Chemical kinetics of water-rock interactions. J. Geophys. Res. Solid Earth 89 (B6), 4009–4025.
Lin, C.Y., Musta, B., Abdullah, M.H., 2013. Geochemical processes, evidence and thermodynamic behavior of dissolved and precipitated carbonate minerals in a modern seawater/freshwater mixing zone of a small tropical island. Appl. Geochem. 29, 13–31.
Neuberger, C.S., Helz, G.R., 2005. Arsenic (III) carbonate complexing. Appl. Geochem. 20 (6), 1218–1225.
Omar, K., Vilcáez, J., 2022. Removal of toxic metals from petroleum produced water by dolomite filtration. J. Water Proc. Eng. 47, 102682.
Pokrovsky, O.S., Schott, J., Thomas, F., 1999. Dolomite surface speciation and reactivity in aquatic systems. Geochem. Cosmochim. Acta 63 (19), 3133–3143.
Ribeiro, L.P.S., Puchala, R., Lalman, D.L., Goetsch, A.L., 2021. Composition of various sources of water in Oklahoma available for consumption by ruminant livestock. Applied Animal Science 37 (5), 595–601.
Ryan, B.H., Kaczmarek, S.E., Rivers, J.M., 2019. Dolomite dissolution: an alternative diagenetic pathway for the formation of palygorskite clay. Sedimentology 66 (5), 1803–1824.
Steefel, C.I., Lasaga, A.C., 1994. A coupled model for transport of multiple chemical species and kinetic precipitation/dissolution reactions with application to reactive flow in single phase hydrothermal systems. Am. J. Sci. 294 (5), 529.
Stumm, W., Morgan, J.J., 1996. Aquatic chemistry. In: Chaps 3 Nad 4. Detailed Systematics of Acid-Base Reactions, the Carbonate System, and Alkalinity Titrations, third ed. Wiley-Interscience, New York.
Temple, B.J., Bailey, P.A., Gregg, J.M., 2020. Carbonate Diagenesis of the Arbuckle Group North Central Oklahoma to Southeastern Missouri, pp. 10–30.
Tesoriero, A.J., Pankow, J.F., 1996. Solid solution partitioning of Sr2+, Ba2+, and Cd2+ to calcite. Geochem. Cosmochim. Acta 60 (6), 1053–1063.
Thompson, J.B., Ferris, F.G., 1990. Cyanobacterial precipitation of gypsum, calcite, and magnesite from natural alkaline lake water. Geology 18, 995e998.

Thompson, J.B., Schultze-Lam, S., Beveridge, T.J., Des Marais, D.J., 1997. Whiting events: biogenic origin due to the photosynthetic activity of cyanobacterial picoplankton. Limnol. Oceanogr. 42, 133e141.
Verrecchia, E.P., Le Coustumer, M.N., 1996. Occurrence and genesis of palygorskite and associated clay minerals in a Pleistocene calcrete complex, Sde Boqer, Negev Desert, Israel. Clay Miner. 31, 183–202.
Vilcáez, J., 2020. Reactive transport modeling of produced water disposal into dolomite saline aquifers: controls of barium transport. J. Contam. Hydrol. 233, 103600.
Wei, H., Shen, Q., Zhao, Y., Wang, D.J., Xu, D.F., 2003. Influence of polyvinylpyrrolidone on the precipitation of calcium carbonate and on the transformation of vaterite to calcite. J. Cryst. Growth 250 (3–4), 516–524.
Wolery, T.J., et al., 1990. Current status of the EQ3/6 software package for geochemical modeling, chemical modeling of aqueous systems II. In: ACS Symposium Series. American Chemical Society, pp. 104–116.